Materials Science and Engineering Publications

Materials Science and Engineering

7-10-2006

In situ transmission electron microscopy study of the nanodomain growth in a Sc-doped lead magnesium niobate ceramic

W. Qu
Iowa State University

X. Zhao
Iowa State University

Xiaoli Tan
Iowa State University, xtan@iastate.edu

Follow this and additional works at: http://lib.dr.iastate.edu/mse_pubs

Part of the Ceramic Materials Commons

The complete bibliographic information for this item can be found at http://lib.dr.iastate.edu/mse_pubs/14. For information on how to cite this item, please visit http://lib.dr.iastate.edu/howtocite.html.

In situ transmission electron microscopy study of the nanodomain growth in a Sc-doped lead magnesium niobate ceramic

Abstract

Sc doping enhances the B-site 1:1 cation ordering in the $Pb(Mg_{1/3}Nb_{2/3})O_3$ ceramic. At low doping levels, the electrical polar domains remain at the nanometer scale and the relaxor ferroelectric behavior persists. The electric field-induced relaxor to normal ferroelectric phase transition process was directly observed with an *in situ* transmission electron microscopy technique in a Sc-doped $Pb(Mg_{1/3}Nb_{2/3})O_3$ polycrystalline sample. It was found that the phase transition started at the grain boundary and took two steps to complete: the gradual coalescence of the polar nanodomains and the abrupt formation of the large wedge-shaped ferroelectric domains.

Keywords

Ozone, Niobium, Ferroelectric phase transitions, Lead, Ceramics, Magnesium, Relaxor ferroelectrics, Transmission electron microscopy, Phase transitions, Polarization

Disciplines

Ceramic Materials | Materials Science and Engineering

In situ transmission electron microscopy study of the nanodomain growth in a Sc-doped lead magnesium niobate ceramic

W. Qu, X. Zhao, and X. Tan

In situ transmission electron microscopy study of the nanodomain growth in a Sc-doped lead magnesium niobate ceramic

W. Qu, X. Zhao, and X. Tan[a)]

Department of Materials Science and Engineering, Iowa State University, Ames, Iowa 50011

Sc doping enhances the *B*-site 1:1 cation ordering in the $Pb(Mg_{1/3}Nb_{2/3})O_3$ ceramic. At low doping levels, the electrical polar domains remain at the nanometer scale and the relaxor ferroelectric behavior persists. The electric field-induced relaxor to normal ferroelectric phase transition process was directly observed with an *in situ* transmission electron microscopy technique in a Sc-doped $Pb(Mg_{1/3}Nb_{2/3})O_3$ polycrystalline sample. It was found that the phase transition started at the grain boundary and took two steps to complete: the gradual coalescence of the polar nanodomains and the abrupt formation of the large wedge-shaped ferroelectric domains. © *2006 American Institute of Physics.* [DOI: 10.1063/1.2219416]

The dielectric property of $Pb(Mg_{1/3}Nb_{2/3})O_3$, the prototype relaxor ferroelectric compound, displays a high relative permittivity, a broad dielectric peak, and a strong frequency dispersion.[1,2] The origin of the relaxor ferroelectric behavior traces back to the structure of the compound, where nanometer scale (<5 nm) 1:1 cation ordering exists on the *B* site of the ABO_3 perovskite.[3–5] In addition to the nanoscale chemical ordering, this compound contains nanoscale polar ordering as well.[6] Despite extensive theoretical and experimental studies for several decades, the relation between these two types of nanoscale ordering is still unclear.[2,7,8]

The polar nanoregions in $Pb(Mg_{1/3}Nb_{2/3})O_3$ can grow into micrometer-sized ferroelectric domains when driven by external electric fields, which correspond to a field-induced first order phase transition.[9–14] Measurements of the field-induced polarization and the x-ray diffraction peak shifts under bias at low temperatures suggested that the phase transition takes place abruptly after an incubation period.[11–13] It is inferred that the polar nanoregions get coarsened during the incubation period.[12,13] However, the morphological evolution of the polar nanodomains during the phase transition has never been directly imaged at the nanometer scale. Furthermore, the time-delayed phase transition has only been observed in high quality pure $Pb(Mg_{1/3}Nb_{2/3})O_3$ single crystals.

Transmission electron microscope (TEM) has long been used to image both polar and chemical nanodomains in relaxor ferroelectric compounds.[3–5] Obviously, TEM equipped with a specimen holder with electrical bias and cooling capabilities would be ideal for studying the electric field-induced relaxor to normal ferroelectric phase transition. As a proof-of-concept for such a study, we explored polycrystalline specimens of a Sc-doped $Pb(Mg_{1/3}Nb_{2/3})O_3$ ceramic. Sc doping was shown to strongly enhance the cation ordering and slightly enhance the polar ordering in $Pb(Mg_{1/3}Nb_{2/3})O_3$ ceramic.[15–17] At low doping levels, large cation ordered domains can be obtained with the relaxor behavior retained. This facilitates the direct observation on the interaction between the chemical domains and the growing polar domains. With the *in situ* TEM technique, we visualized the electric field-induced phase transition process in a relaxor ferroelectric compound at the nanometer scale.

The Sc dopant is incorporated through solid solution of $Pb(Mg_{1/3}Nb_{2/3})O_3$ with $Pb(Sc_{1/2}Nb_{1/2})O_3$. The composition of the ceramic used in this study is $0.92Pb(Mg_{1/3}Nb_{2/3})O_3-0.08Pb(Sc_{1/2}Nb_{1/2})O_3$ (abbreviated as PSMN8). A two step solid state reaction method was employed to prepare the ceramic. The starting materials used in this work were commercially available and high purity (better than 99.9 wt %) PbO, MgO, Nb_2O_5, and Sc_2O_3 powders. After vibratory milling in isopropyl alcohol for 6 h and subsequent drying, the well-mixed stoichiometric powders of *B*-site oxides were calcined at 1100 °C for 4 h. The calcined powders were then combined with PbO powder, milled for 6 h, and calcined at 900 °C for 4 h to form phase pure perovskite powder. Pressed disks, 12 mm in diameter by 2 mm thick, were formed by cold pressing. The preformed pellets were then sintered at 1250 °C for 3 h and cooled slowly to 900 °C at the rate of 10 °C/h in controlled atmosphere.

The surface layers of the sintered pellets were removed and x-ray diffraction was used to check the phase purity and the cation ordering. The cation ordering was also examined by dark field imaging in a JEOL 2010 TEM, operating at 200 keV. The dielectric characterization was performed with an *LCR* meter (HP-4284A, Hewlett-Packard) in conjunction with an environmental chamber (9023, Delta Design). A cooling rate of 2 °C/min was used during this measurement. Electric field-induced phase transition was then evaluated by the thermal depolarization measurement with a picoammeter (Model 484, Keithley) and the polarization hysteresis measurement with a standardized ferroelectric test system (RT-66A, Radiant technologies). The *in situ* TEM experiment was carried out on the same JEOL 2010 TEM with a special specimen holder. The holder has two electrical leads at the tip and the specimen can be cooled by liquid nitrogen. Detailed specimen preparation procedure and electrode configuration for the *in situ* study can be found in previous reports.[18–20] Starting at room temperature, an electrical voltage of 200 V, corresponding to a field of 10 kV/cm, was applied and maintained. The specimen was then cooled at a rate of 2 °C/min. Bright/dark field images as well as selected area electron diffraction patterns were recorded by a charge-coupled device (CCD) camera at certain temperatures.

X-ray diffraction showed an evident $\left(\frac{1}{2}\frac{1}{2}\frac{1}{2}\right)$ superlattice peak which indicates a strong 1:1 *B*-site cation ordering. The
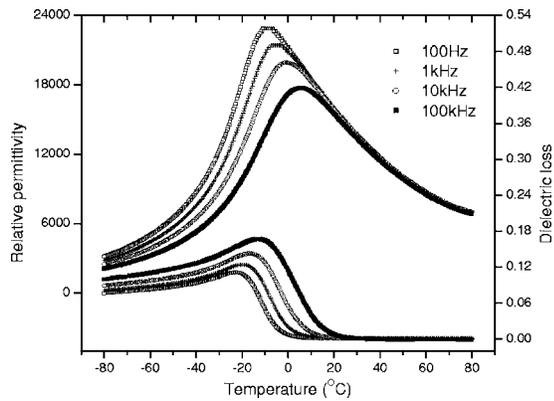
a)Electronic mail: xtan@iastate.edu

FIG. 1. Relative dielectric permittivity and dielectric loss as a function of temperature in the PSMN8 ceramic at 0.1, 1, 10, and 100 kHz.

FIG. 2. Electric field-induced polarization measurement at 4 Hz of a bulk circular plate sample and an unperforated TEM specimen.

ordering parameter α for the ceramic, evaluated according to the common procedure used in literature,[15] is 0.9. The x-ray diffraction also indicated a pseudocubic structure with a lattice parameter of 4.0608 Å. Compared with the lattice parameter of 4.0509 Å for the undoped $Pb(Mg_{1/3}Nb_{2/3})O_3$, Sc doping increased the unit cell size due to the larger Sc^{3+} ion radius. The strong 1:1 cation ordering in the ceramic is further confirmed by TEM analysis. Chemical domains with average size on the order of 100 nm were clearly seen.

The dielectric properties of the ceramic are shown in Fig. 1. The permittivity exhibits characteristics of a relaxor ferroelectric, namely, a broad peak and a strong frequency dispersion. At 1 kHz, the maximum relative permittivity ε_{max} was measured as 21 441 at the T_{max} of -5 °C. The thermal depolarization measurement was carried out on a sample during zero-field heating after it had been cooled under a field of 10 kV/cm. The T_{d0} was measured to be -38 °C. Compared with the T_{max} of -10 °C and the T_{d0} of -60 °C in pure $Pb(Mg_{1/3}Nb_{2/3})O_3$,[10] Sc doping shifts both T_{max} and T_{d0} to higher temperatures, indicative of an enhanced ferroelectric polar order. In accordance with this, the ε_{max} decreases slightly compared to that of the undoped $Pb(Mg_{1/3}Nb_{2/3})O_3$ ceramic (22 870 at 1 kHz).

The electric field-induced relaxor to normal ferroelectric phase transition in the ceramic was characterized by the polarization hysteresis measurement on a bulk circular plate sample with diameter of 10 mm and thickness of 0.2 mm, with the field applied along the thickness direction. As expected, at room temperature, the PSMN8 ceramic showed a nonlinear $P \sim E$ relation with no hysteresis, as shown in Fig. 2. However, a well-defined square hysteresis loop was observed at -50 °C, with coercive field E_c of 5.2 kV/cm and remanent polarization P_r of 26 μC/cm². Further decreasing in temperature leads to the increase in both E_c and P_r. The appearance of the square hysteresis loops at low temperatures indicates the presence of a normal ferroelectric phase in PSMN8.

In order to determine the field level needed for the *in situ* TEM study and assess the sample geometry effect on the field-induced phase transition, a TEM specimenlike sample (a 100 μm thick disk with diameter of 3 mm) was tested for the hysteresis measurement too. In this configuration, two half-circle shaped electrodes were deposited on a flat surface of the disk with a gap of 200 μm.[18–20] Therefore, in-plane electric fields were applied and the result is also plotted in Fig. 2. Compared to the conventional circular plate sample
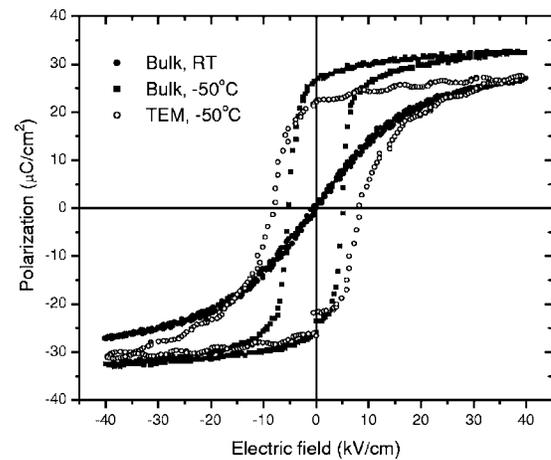
with electric field applied along the thickness direction, the TEM specimenlike disk shows a higher E_c (8.2 kV/cm) and a lower remanent polarization. Furthermore, the hysteresis loop is no longer symmetrical.

The electric field-induced phase transition was then directly visualized inside a TEM on a specimen during a cooling process under 10 kV/cm static electric field, as shown in Fig. 3. One grain with its $\langle 110 \rangle$ direction close to the electron beam was focused. Strong cation ordering was observed with dark field imaging in this grain. At room temperature, very faint contrast of polar nanoregions, associated with bending contours, is noticed [Fig. 3(a)]. The inset in Fig. 3(a) shows the $\langle 110 \rangle$ zone-axis electron diffraction pattern. The in-plane directions $\langle 001 \rangle$ and $\langle 1\bar{1}0 \rangle$ are indicated by bright arrows in this micrograph. A grain boundary is also noted by the bright dashed line at the top.

Then the polycrystalline specimen was subjected to a field-cooling process, with the direction indicated by the bright arrow in Fig. 3(b). The field direction happened to be very close to the $\langle 001 \rangle$ direction. No detectable morphological changes of the polar nanoregions were observed at room temperature under the static field. However, when the temperature reached -50 °C, evident changes were noticed in the area close to the grain boundary, as shown in Fig. 3(b). It is clear that clustering of the polar nanoregions occurred. The coalescence of the polar nanodomains continued during the further cooling to -55 °C [Fig. 3(c)]. Up to this temperature, the morphology of the nanodomains remained irregular shaped without well-defined domain walls. When the temperature reached -70 °C, a dramatic change in the domain morphology was observed [Fig. 3(d)]. Large wedge-shaped ferroelectric domains (>200 nm) with straight domain walls appeared in the close vicinity of the grain boundary. The domain walls are close to the $\{1\bar{1}0\}$ plane. Further cooling to -90 °C led to the growth of existing large domains and the emergence of additional large domains [Fig. 3(e)]. At this temperature (-90 °C), the specimen was held for 30 min under the applied bias. Further growth of the large domains was seen [Fig. 3(f)].

The results shown in Fig. 3 indicate that there are two stages for the evolution of the polar nanodomains under electric field, the gradual coalescence of nanodomains and the abrupt formation of wedge-shaped large domains. This observation is very similar to the transition process depicted by
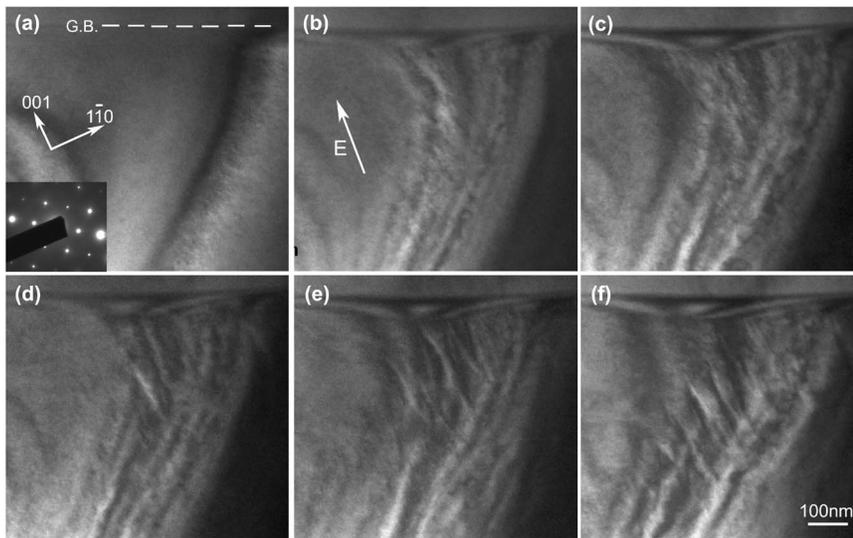
FIG. 3. The morphological evolution of the polar nanodomains during field-cooling under 10 kV/cm revealed by the *in situ* TEM technique. The applied field direction is shown by the arrow in (b). (a) The initial polar nanoregions at room temperature. The inset shows the $\langle 110 \rangle$ zone-axis selected area electron diffraction (SAED) pattern. (b) −50 °C, (c) −55 °C, (d) −70 °C, (e) −90 °C, and (f) −90 °C after 30 min.

x-ray diffraction and polarization measurement in $\langle 111 \rangle$-oriented $Pb(Mg_{1/3}Nb_{2/3})O_3$ single crystals.[12,13] It should be noted that the current observation was made with one individual grain in a polycrystalline ceramic. It implies that the field-induced phase transition behavior of individual grains in a polycrystalline aggregate resembles that of single crystals. However, the macroscopic polarization measurement in polycrystalline ceramics was not able to reveal the two-stage process.

Figure 3 also shows that the coalescence of polar nanodomains and the formation of wedge-shaped large domains take place in the vicinity of a grain boundary. The result is consistent with the random field model for relaxor ferroelectrics, where the polar ordering is controlled by the quenched random electric fields originating from charged point defects.[21] At grain boundaries, higher concentration of point defects is expected. Therefore, grain boundaries are preferred sites for the initiation of the field-induced phase transition.

The electric field-induced normal-ferroelectric phase presumably possesses a rhombohedral structure with spontaneous polarization along the $\langle 111 \rangle$.[10] Under current experimental conditions, the electric field is applied along a direction close to the $\langle 001 \rangle$. Therefore, domains with polarization vectors $[111]$, $[1\bar{1}1]$, $[\bar{1}11]$, and $[\bar{1}\bar{1}1]$ should be almost equally favored and multiple domains are expected. This is indeed the case as confirmed in Fig. 3. The observed $\{1\bar{1}0\}$ domain walls are therefore electrically charged. It should be pointed out here that there is an alternative interpretation of these domain walls. Close examination of Figs. 3(e) and 3(f) shows that the multiple domains may merge to a single domain as they grow. Therefore, these domain walls could possibly be the rhombohedral/pseudocubic phase boundary.

To summarize, strong 1:1 *B*-site cation ordering is present in the $0.92\,Pb(Mg_{1/3}Nb_{2/3})O_3$ $-0.08\,Pb(Sc_{1/2}Nb_{1/2})O_3$ solid solution. This chemically ordered ceramic retains the characteristics of the relaxor behavior but with an enhanced ferroelectric polar order. At lower temperatures, a relaxor to normal ferroelectric phase transition can be triggered by external electric fields. Direct observation with an *in situ* TEM technique reveals that the phase transition process is initiated at the grain boundary. The polar nanoregions gradually coalesce and then abruptly transform into wedge-shaped large ferroelectric domains. The large domains merge into a single domain as they grow.

[1] G. A. Smolensky, J. Phys. Soc. Jpn. **28**, 26 (1970).
[2] L. E. Cross, Ferroelectrics **76**, 241 (1987).
[3] J. Chen, H. M. Chan, and M. P. Harmer, J. Am. Ceram. Soc. **72**, 593 (1989).
[4] A. D. Hilton, D. J. Barber, C. A. Randall, and T. R. Shrout, J. Mater. Sci. **25**, 3461 (1990).
[5] Z. Xu, S. M. Gupta, D. Viehland, Y. Yan, and S. J. Pennycook, J. Am. Ceram. Soc. **83**, 181 (2000).
[6] G. Burns and F. H. Dacol, Solid State Commun. **48**, 853 (1983).
[7] Z. G. Ye, Key Eng. Mater. **155–156**, 81 (1998).
[8] B. P. Burton, E. Cockayne, and U. V. Waghmare, Phys. Rev. B **72**, 064113 (2005).
[9] H. Arndt, F. Sauerbier, G. Schmidt, and L. A. Shebanov, Ferroelectrics **79**, 145 (1988).
[10] Z. G. Ye and H. Schmid, Ferroelectrics **145**, 83 (1993).
[11] E. V. Colla, E. Y. Koroleva, N. M. Okuneva, and S. B. Vakhrushev, Phys. Rev. Lett. **74**, 1681 (1995).
[12] S. B. Vakhrushev, J. M. Kiat, and B. Dkhil, Solid State Commun. **103**, 477 (1997).
[13] B. Dkhil and J. M. Kiat, J. Appl. Phys. **90**, 4676 (2001).
[14] B. E. Vugmeister and H. Rabitz, Phys. Rev. B **65**, 024111 (2002).
[15] L. Farber, M. Valant, M. A. Akbas, and P. K. Davies, J. Am. Ceram. Soc. **85**, 2319 (2002).
[16] L. Farber and P. K. Davies, J. Am. Ceram. Soc. **86**, 1861 (2003).
[17] X. Zhao, W. Qu, H. He, N. Vittayakorn, and X. Tan, J. Am. Ceram. Soc. **89**, 202 (2006).
[18] Z. Xu, X. Tan, P. Han, and J. K. Shang, Appl. Phys. Lett. **76**, 3732 (2000).
[19] H. He and X. Tan, Appl. Phys. Lett. **85**, 3187 (2004).
[20] X. Tan, H. He, and J. K. Shang, J. Mater. Res. **20**, 1641 (2005).
[21] V. Westphal, W. Kleemann, and M. D. Glinchuk, Phys. Rev. Lett. **68**, 847 (1992).